ADEQUACY OF SURFACE DIFFUSION MODELS TO SIMULATE NONEQUILIBRIUM MASS TRANSFER IN SOILS

By

NAZMUL HASAN

A thesis submitted in partial fulfillment of
the requirements for the degree of

Masters of Science in Environmental Engineering

WASHINGTON STATE UNIVERSITY
Department of Civil and Environmental Engineering

AUGUST 2008

To the Faculty of Washington State University:

The members of the Committee appointed to examine the thesis of NAZMUL HASAN find it satisfactory and recommend that it be accepted.

_____
Chair

_____

_____

ACKNOWLEDGEMENTS

This thesis would not have been possible without the support of some people.

I would like to thank my supervisor Professor Dr. Akram Hossain . He provided a unique perspective and invaluable guidance to this work. His wisdom, encouragement, and time investment are very much appreciated. I am very grateful to him.

I also thank my committee members Dr. Ken Hartz, Dr. James B. Duncan for their time and suggestions.

I would also like to thank my parents, family and friends for their constant encouragement and emotional support. Finally I would like to thank Amena Moth Mayenna for her great support and help through the entire work.

ADEQUACY OF SURFACE DIFFUSION MODELS TO SIMULATE

NONEQUILIBRIUM MASS TRANSFER IN SOILS

Abstract

by NAZMUL HASAN,
Washington State University
AUGUST 2008

Chair: Akram Hossain.

Diffusion from intraparticle pore spaces is considered to be the main reason for slow release of contaminants from soil. Diffusion controlled mass transfer can be simulated by the homogeneous surface diffusion model (HSDM). The objective of this paper is to present a simplified HSDM model (SHSDM) and a finite element HSDM model (FEHSDM) to simulate advective-dispersive transport through soils, coupled with intraparticle diffusion, under nonequilibrium conditions and compare these models with the dispersed flow, film and particle diffusion model (DF-FPDM) that has recently been reported in literature. The models, by and large, provide convergent results and remain stable for Peclet number $\mathrm{Pe} \le 2.5$ and Courant number $\mathrm{Cr} \le 1.0$. The SHSDM and the DF-FPDM predictions are practically the same for mass transfer Biot number $\mathrm{Bi} \ge 5$. However, considerable difference in the predictions of these two models are observed for $\mathrm{Bi} \le 1$. The FEHSDM predictions compare well with experimental data for slightly hydrophobic compounds. The SHSDM and the DF-FPDM predictions, on the other hand, compare well with experimental results for relatively hydrophobic compounds.

TABLE OF CONTENTS

Page

LIST OF TABLES

LIST OF FIGURES

INTRODUCTION

Contaminant, especially hydrocarbons, release from soil normally occurs under nonequilibrium conditions and may require long time for it to be fully released (Ball and Roberts, 1991; Loehr and Webster, 1996; Loehr et al., 2000). The slow release has been attributed to a rate-limiting diffusion mechanism (Grathwohl and Reinhard, 1993; Pignatello et al., 1993). Diffusion from intraparticle pore spaces of soil particles is considered to be the main reason for this slow release (Niedermeier and Loehr, 2005).

Diffusion models have been employed extensively to describe sorption kinetics of hydrophobic chemical in soil particles (Ball and Roberts, 1991; Grathwohl and Reinhard, 1993; Cornelissen, 1998; Farell et al., 1999; Kleineidam et al., 1999; Rahman et al., 2003; Worch, 2004). Solution of intraparticle diffusion equation coupled with advective-dispersive transport can be quite challenging.

The homogeneous surface diffusion model (HSDM) has been used successfully for more than 100 adsorption systems (Weber and Pirbazari, 1982). Rahman et al. (2003) presented a nonequilibrium mass transfer model employing a simplified mathematical description of the HSDM. The model was referred to as "dispersed flow, film and particle diffusion model (DF-FPDM)". The model appeared to adequately predict experimentally developed adsorption breakthrough data for a continuous source. Rahman et al. (2003) obtained dispersivity values from independent tracer tests which were then adjusted to achieve better fit of the model predictions with the experimental data. Adjustments in adsorption and intraparticle mass transfer coefficients were made by Worch (2004) to obtain a better fit between the DF-FPDM prediction

and experimental results. It is, therefore, essential that the DF-FPDM's ability to predict nonequilibrium mass transfer for different conditions is further examined.

Hand et al. (1984) presented analytical solutions of a simplified HSDM to predict adsorption of contaminants onto porous media. These analytical solutions, however, can not be employed to simulate desorption and such a model is of limited utility in predicting nonequilibrium mass transport in soils. As mentioned, the HSDM has been used successfully to simulate over 100 adsorption systems. Consequently, a number of mathematical models are available. Thacker (1981) presented an excellent numerical model, based on the method of orthogonal collocation (MOC), to simulate sorption by fixed-bed adsorbers. An inspection of the computer code presented by Thacker (1981) leads to the conclusion that the model might have suffered from numerical instability under certain system conditions. Similar observation was made in the excellent work presented by Liang (1984), which was based on a finite difference method (FDM).

FDMs are commonly employed to solve advective-dispersive transport coupled with intraprticle diffusion (Sun and Meunier, 1991). FDMs, however, require strict conditions for stability (Thibaud-Erkey et al., 1996). Fast Fourier transform (FFT) can be used when sorption characteristics is linear (Chen and Hsu, 1987). Often times, however, sorption characteristics are nonlinear as mentioned. A MOC was employed by Raghavan and Ruthven (1993) to solve similar problems with nonlinear sorption characteristics. The MOC, nonetheless, can fail due to numerical oscillations (Thibaud-Erkey et al., 1996).

Finite element models (FEMs) are currently gaining popularity in simulating contaminant

transport. Hossain and Yonge (1992) presented an "upwind" Galerkin FEM (UGFEM) to simulate advective transport of contaminants nonlinearly coupled with intraparticle diffusion through fixed-bed activated carbon columns. The UGFEM was found to be stable and convergent for a wide range of system conditions. Further, the model offered computational efficiency over the method of MOC. The model did not, however, include the effect of dispersion. Further, an "upwind" model is known to provide numerical stability at the expense of artificial dispersion. FEMs without upwinding employing HSDM for simulating intraparticle diffusion should be developed to examine their suitability in simulating nonequilibrium mass transfer in soils. This model will be referred to as the finite element HSDM (FEHSDM).

Numerical experimentation with a model revealed that the dimensionless liquid-phase contaminant concentration in the hydrodynamic boundary layer around a particle closely follows that in the inter-particle pore spaces for a wide range of system conditions. The film transfer resistance can, therefore, be neglected in such a case. If film transfer resistance is neglected then the contaminant in the inter-particle pore spaces can be considered in equilibrium with the contaminant on the particle surface. A model simulating this simplified condition may provide computational advantage over the other available models. This simplified model will be referred to as the simplified HSDM (SHSDM).

The objective of this paper is to present details of the SHSDM, the FEHSDM and compare their predictive ability with that of the DF-FPDM for a wide range of system conditions. Additionally, the paper presents criteria for convergence and stability for the models.

THE MODELS

The SHSDM

Model Equations

The advective-dispersive transport through inter-particle pore spaces and intra-particle diffusion of contaminants into the soil solids for the SHSDM can be described by the following equations.

$$\frac{\partial C}{\partial t} = -v\frac{\partial C}{\partial x} + D\frac{\partial^2 C}{\partial x^2} - \frac{\rho_b}{\varepsilon}\frac{\partial q}{\partial t} \qquad (1)$$

$$\frac{dq}{dt} = k_S a_V (q_S - q) \qquad (2)$$

In the above equations, C is the contaminant concentration in the inter-particle pore spaces (ML^{-3}), t is the time (T), v is the velocity of flow through the inter-particle pore spaces (LT^{-1}), x is the distance along the direction of the flow (L), D is the dispersion coefficient (L^2T^{-1}), q is the concentration of the contaminant in the soil solid (MM^{-1}), ρ_b is the bulk density of the soils (ML^{-3}), ε is the porosity, k_s is the intra-particle mass transfer coefficient (L^2T^{-1}), a_V is the mass transfer area per unit volume (L^2L^{-3}), and q_s is the concentration of the contaminant on the surface of the soil solids (MM^{-1}) which is being assumed to be in equilibrium with C.

Eq. (1) that describes transport through the inter-particle pore spaces can be subjected to the following initial and boundary conditions.

$$t = 0, \quad 0 < x \le L, \quad C = 0 \qquad (3)$$

$$t \geq 0, \quad x = 0, \quad C = C_0(t) \tag{4}$$

$$t \geq 0, \quad x = L, \quad \frac{\partial C}{\partial x} = 0 \tag{5}$$

In the above equations, L is the length of the flow field under consideration and $C_0(t)$ is the source concentration.

Eq. (2), on the other hand, describes transport of contaminants in the intra-particle pore spaces and is subjected to the following initial conditions.

$$t = 0 \quad q = q_S = 0 \tag{6}$$

The liquid phase concentration of the contaminant, C, is assumed to be in equilibrium with the solid phase concentration q_s and the equilibrium relationship can be expressed by the following equation.

$$q_s = kC^n \tag{7}$$

Here k and n are constants specific to the soil and the contaminant of concern.

Dimensionless Model

Eqs. (1-2) and the associated boundary and initial conditions were converted to the following dimensionless forms by employing dimensionless variables introduced by Rahman et al. (2003).

$$\frac{\partial \overline{C}}{\partial \overline{x}} + \frac{\partial \overline{q}}{\partial \overline{t}} = 0 \tag{8}$$

$$\frac{d\overline{q}}{d\overline{t}} = \beta\left(\overline{q}_s - \overline{q}\right) \tag{9}$$

$$\overline{t} = 0, \quad 0 < \overline{x} \le 1, \quad \overline{C} = 0, \quad \overline{q} = 0 \tag{10}$$

$$\overline{t} \ge 0, \quad \overline{x} = 0, \quad \overline{C} = \overline{C}_0\left(\overline{t}\right) \tag{11}$$

$$\overline{q}_s = \overline{C}^n \tag{12}$$

In deriving Eq. (8), the dispersion term was not considered. The effect of dispersion was incorporated by modifying k_S assuming that surface diffusion and longitudinal dispersion operate in series analogous to external mass transfer coefficient modification by Rahman et al. (2003).

The dimensionless variables and parameters used in Eqs. (8 – 12), even though, can be found elsewhere (Rahman et al., 2003; Worch, 2004), are given below for reference.

$$\overline{C} = \frac{C}{C_0}; \ \overline{q}_s = \frac{q_s}{q_e}; \ \overline{q} = \frac{q}{q_e} \tag{13 – 15}$$

$$\overline{x} = \frac{x}{L}; \ \overline{t} = \frac{t}{\tau}; \ \tau = \frac{L}{v}\left(1 + \frac{q_e \rho_b}{C_0 \varepsilon}\right); \ \beta = k_s a_v \tau \tag{16 – 19}$$

Solution Technique

Temporal and spatial derivatives in Eqs. (8 – 9) were discretized implicitly by backward finite difference schemes to obtain the following equations.

$$\overline{C}_i^{\bar{t}} = \frac{\eta_1(1+\eta_2)\overline{C}_{i-1}^{\bar{t}}}{\eta_1(1+\eta_2)+\eta_2} + \frac{\eta_2\overline{q}_i^{\bar{t}-\Delta\bar{t}}}{\eta_1(1+\eta_2)+\eta_2} \quad (20)$$

$$\overline{q}_i^{\bar{t}} = \frac{\eta_2\overline{C}_i^{\bar{t}}}{1+\eta_2} + \frac{\overline{q}_i^{\bar{t}-\Delta\bar{t}}}{1+\eta_2} \quad (21)$$

In Eqs. (20 – 21), $\Delta\bar{t}$ is the length of the time step and i is the node number. Parameters associated with Eqs. (20 – 21) are defined below.

$$\eta_1 = \frac{\Delta\bar{t}}{\Delta\bar{x}};\ \eta_2 = \frac{\alpha\beta}{\alpha\beta+L}\Delta\bar{t} \quad (22-23)$$

In Eq. (22 – 23), $\Delta\bar{x}$ is the node to node distance and α is the dispersivity (L). Eqs. (20 – 21) can be used to find contaminant concentration, in the inter-particle pore space and in the solid phase, by utilizing the initial and the boundary conditions.

The DF-FPDM

Model Equations

The DF-FPDM presented by Rahman et al. (2003) can be described by Eqs. (1 – 6) of the SHSDM and the following equations.

$$\frac{dq}{dt} = \frac{k_f a_V}{\rho_b}(C - C_S) \quad (24)$$

$$q_s = kC_S^n \quad (25)$$

In the above equations, k_f is the film transfer coefficient $\left(LT^{-1}\right)$, and C_s is the concentration of contaminants in the boundary layer surrounding a particle $\left(ML^{-3}\right)$. In DF-FPDM, concentration of the contaminant, C_s, in the boundary layer is assumed to be in equilibrium with the solid phase concentration q_s.

Dimensionless Model

The dimensionless DF-FPDM can be described by Eqs. (8-11, 13-19) and the following equations.

$$\frac{d\overline{q}}{d\overline{t}} = \gamma\left(\overline{C} - \overline{C}_S\right) \tag{26}$$

$$\overline{q}_s = \overline{C}_S^n \tag{27}$$

The dimensionless parameter γ is defined below and the rest of the dimensionless parameters are the same as those in the SHSDM.

$$\gamma = \frac{k_f a_V \tau C_0}{\rho_b q_e} \tag{28}$$

Solution Technique

Eqs. (8-9, 26) were implicitly discretized by employing backward finite difference scheme to obtain the following equations for linear adsorption.

$$\overline{C}_i^{\bar{t}} = \frac{\xi_1}{\xi}\overline{C}_{i-1}^{\bar{t}} + \frac{\xi_2}{\xi}\overline{q}_i^{\bar{t}-\Delta\bar{t}} - \frac{\xi_3}{\xi}\left(\overline{C}_i^{\bar{t}-\Delta\bar{t}} - \overline{C}_{i-1}^{\bar{t}-\Delta\bar{t}}\right) \tag{29}$$

$$\overline{C}_{Si}^{\bar{t}} = \frac{\zeta_1}{\xi}\overline{C}_{i-1}^{\bar{t}} + \frac{\zeta_2}{\xi}\overline{q}_i^{\bar{t}-\Delta\bar{t}} + \frac{\zeta_3}{\xi}\left(\overline{C}_i^{\bar{t}-\Delta t} - \overline{C}_{i-1}^{\bar{t}-\Delta\bar{t}}\right) \tag{30}$$

$$\overline{q}_i^{\bar{t}} = \overline{q}_i^{\bar{t}-\Delta\bar{t}} - \eta_1\left(\overline{C}_i^{\bar{t}} - \overline{C}_{i-1}^{\bar{t}}\right) - \eta_1\left(\overline{C}_i^{\bar{t}-\Delta\bar{t}} - \overline{C}_{i-1}^{\bar{t}-\Delta\bar{t}}\right) \tag{31}$$

The dimensionless parameters utilized in the preceding equations are defined below.

$$\xi = \eta_3(\eta_1 + \omega) + \eta_1\omega(1 + \eta_3) \tag{32}$$

$$\xi_1 = \eta_1\omega(1 + \eta_3) + \eta_1\eta_3 \tag{33}$$

$$\xi_2 = \eta_1\eta_3 \tag{34}$$

$$\xi_3 = \eta_1\omega(1 + \eta_3) + \eta_1\eta_3 \tag{35}$$

$$\zeta_1 = \eta_1(\eta_1 + \omega)(1 + \eta_3) - \eta_1^2(1 + \omega) \tag{36}$$

$$\zeta_2 = \eta_3(\eta_1 + \omega) \tag{37}$$

$$\zeta_3 = \eta_1^2(1 + \omega) - \eta_1(\eta_1 + \omega)(1 + \eta_3) \tag{38}$$

$$\eta_3 = \frac{\alpha\gamma}{\alpha\gamma + L}\Delta\bar{t} \tag{39}$$

Eqs. (29 – 31) can be used to find contaminant concentration in the inter-particle pore space, in the boundary layer, and in the solid phase by utilizing associated initial and the boundary conditions.

The FEHSDM

Model Equations

If soil particles are assumed spherical and homogeneous surface diffusion of contaminants is considered for intra-particle transport, the following equations describe the FEHSDM.

$$\frac{\partial C}{\partial t} = -v\frac{\partial C}{\partial x} + D\frac{\partial^2 C}{\partial x^2} - 3\frac{k_f}{R}\frac{1-\varepsilon}{\varepsilon}\left(C - C_s\right) \tag{40}$$

$$\frac{\partial q}{\partial t} = \frac{D_s}{r^2}\frac{\partial}{\partial r}\left(r^2\frac{\partial q}{\partial r}\right) \tag{41}$$

In the above equations, R is the radius of a particle (L) and r is the radial distance from the center of a particle (L).

Eq. (40) describes transport through the inter-particle pore spaces and can be subjected to the initial and boundary conditions in Eqs. (3 – 5). Eq. (41) describes transport of contaminants in the intra-particle pore spaces. It can be subjected to the following initial and boundary conditions:

$$t = 0 \quad 0 \le r < R, \quad q = 0 \tag{42}$$

$$t \ge 0, \quad r = 0, \quad \frac{\partial q}{\partial r} = 0 \tag{43}$$

$$t \ge 0, \quad r = R, \quad D_s\rho_b\frac{\partial q}{\partial r} = k_f\left(C - C_s\right) \tag{44}$$

Contaminant concentration, C_s, in the boundary layer is assumed to be in equilibrium with the

solid phase concentration q_s and can be described by Eq. (25).

Dimensionless Equations

The model equations were converted to their respective dimensionless forms by introducing dimensionless variables to minimize computational difficulty inherent to the numerical solution of the coupled advective-dispersive transport equation and the intra-particle diffusion equation. Dimensionless forms of Eqs. (40 – 41) and associated initial and boundary conditions are presented below.

$$\frac{\partial \overline{C}}{\partial \bar{t}} = -D_g \frac{\partial \overline{C}}{\partial \bar{x}} + \frac{D_g}{P_e} \frac{\partial^2 \overline{C}}{\partial \bar{x}^2} - 3D_g St(\overline{C} - \overline{C}_s) \tag{45}$$

$$\bar{r}^2 \frac{\partial \bar{q}}{\partial \bar{t}} = E_d \frac{\partial}{\partial \bar{r}} \left[\bar{r}^2 \frac{\partial \bar{q}}{\partial \bar{r}} \right] \tag{46}$$

$$\bar{t} = 0, \quad 0 < \bar{x} \le 1, \quad \overline{C} = 0 \tag{47}$$

$$\bar{t} \ge 0, \quad \bar{x} = 0, \quad \overline{C} = \overline{C}_0(\bar{t}) \tag{48}$$

$$\bar{t} \ge 0, \quad \bar{x} = 1, \quad \frac{\partial \overline{C}}{\partial \bar{x}} = 0 \tag{49}$$

$$\bar{t} = 0 \quad 0 \le \bar{r} < 1, \quad \bar{q} = 0 \tag{50}$$

$$\bar{t} \ge 0, \quad \bar{r} = 0, \quad \frac{\partial \bar{q}}{\partial \bar{r}} = 0 \tag{51}$$

$$\bar{t} \ge 0, \quad \bar{r} = 1, \quad \frac{\partial \bar{q}}{\partial \bar{r}} = Sh\left(\overline{C} - \overline{C}_s\right) \tag{52}$$

$$\bar{r} = 1, \quad \bar{q}_s = \overline{C}_s^{\,n} \tag{53}$$

The dimensionless variables, not defined in the preceding sections, are presented below.

$$\bar{r} = \frac{r}{R};\ \tau_1 = \frac{L}{v};\ D_g = \rho \frac{q_e}{C_0} \frac{1-\varepsilon}{\varepsilon} \qquad (54-56)$$

$$\bar{t} = \frac{t}{\tau_1 D_g};\ Pe = \frac{vL}{D};\ St = \frac{k_f \tau_1 (1-\varepsilon)}{\varepsilon R} \qquad (57-59)$$

$$E_d = \frac{\tau_1 D_g D_s}{R^2};\ Sh = \frac{R k_f C_0}{D_s \rho q_e} \qquad (60-61)$$

Solution Technique

The dimensionless equations were discretized by employing piecewise linear basis functions and the Crank-Nicolson Galerkin minimization principle to obtain a set of ordinary equations (ODEs) in time. The ODEs in time were then further discretized by employing the backward difference formula to obtain a set of linear algebraic systems (LAS). The LAS was then solved at each time step by utilizing associated boundary and initial conditions.

CONVEREGENCE AND STABILITY

The SHSDM and the DF-FPDM, in general, provide convergent results for Peclet number $Pe = \frac{v\Delta x}{D} \le 2.5$ and Courant number $Cr = \frac{v\Delta t}{\Delta x} \le 1.0$. Numerical stability is not a concern here because explicit algebraic expressions have been developed for the solutions of these two models. The FEHSDM provides convergent results for $Pe \le 2.5$ and $Cr \approx 1.0$, and was determined to be stable by the von Neumann method for this condition. However, finer temporal and spatial discretizations may be needed for certain conditions to avoid oscillation in the solution of the advective-dispersive transport equation (Eq. 45). Oscillation may result in negative liquid phase

concentration resulting in the breakdown of the algorithm.

EFFECT OF MICROTRANSPORT PARAMETERS

The microtransport parameters are the film transfer coefficient k_f and the diffusion coefficient D_S. Effect of microtransport parameters on mass transport can be evaluated by computing the mass transfer Biot number, Bi, as defined below.

$$Bi = \frac{k_f R(1-\varepsilon)C_0}{\rho_b D_S q_e} \tag{62}$$

A Bi of greater than 30 implies that surface diffusion controls and a Bi of less than 0.50 is an indication of film transfer limited transport (Weber and Digiano, 1995).

Numerical experiments have shown that the SHSDM predictions differ significantly from those of the DF-FPDM for $Bi \le 1$. Fig. 1 presents the model predictions for $Bi = 1$. An examination of Fig. 1 reveals a significant difference between the SHSDM and the DF-FPDM predicted breakthrough curves (BTCs). The difference gets more significant as Bi becomes smaller than 1. However, these two predictions virtually become the same for $Bi \ge 5$. Model predictions for $Bi = 5$ is presented in Fig. 2 for reference. The FEHSDM predictions were always found to differ from the other two models.

MODEL PREDICTIONS VERSUS EXPERIMENTAL RESULTS

Adsorption

Experimental BTCs, for adsorption in soil columns, were obtained from literature (Rahman et al., 2003) for 2-methyl-4,6-dinitrophenol (2-M-4,6-DNP), 2,4,6-trichlorophenol (2,4,6-TCP), phenanthrene, and pentachlorophenol (PCP) to utilize in evaluating the relative accuracy of the models. The model parameters were also obtained from Rahman et al. (2003) and are presented in Table 1.

Comparisons of model predictions and experimental results for 2-M-4,6-DNP and 2,4,6-TCP are presented in Figs. 3 and 4, respectively. These two compounds are only slightly hydrophobic as evidenced from isotherm constant k presented in Table 1. The FEHSDM better predicts the breakthrough times and the first halves of the rising portions of the BTCs in both cases. Furthermore, the FEHSDM, in general, can be considered in better agreement with the experimental results than the DF-FPDM and the SHSDM.

Biot number for 2-M-4,6-DNP was computed to be 1435. It was 1136 for 2,4,6-TCP. Therefore, overall mass transfer is diffusion limited for both the contaminants. The SHSDM assumes a diffusion limited mass transport. Therefore, the SHSDM prediction should have been very similar to that of the FEHSDM. The lack of similarity can be explained by the fact that the SHSDM equations are different than those of the FEHSDM. Further, the SHSDM predictions are very similar to those by the DF-FPDM in both cases which is expected for $Bi \geq 5$ as explained in the preceding section.

Model predictions and experimental BTCs for phenanthrene and PCP are presented in Figs. 5 and 6, respectively. These two compounds are significantly hydrophobic as evidenced from their isotherm constant k contained in Table 1. A Bi of 3958 was computed for phenanthrene and a Bi of 5 was computed for PCP. Consequently, the SHSDM and the DF-FPDM are virtually the same in Figs. 5 and 6. Further, the SHSDM and the DF-FPDM predictions are in better agreement with the experimental BTCs than the FEHSDM prediction.

Adsorption Followed by Desorption

Adsorption followed by desorption is of significant practical interest. Experimental BTCs for chlorobenzene (CBENZ) and trichloroethene (TCE) were obtained from literature (Hu and Brusseau, 1996). Figs. 7 and 8 present comparisons of the model predictions, obtained by utilizing the parameters contained in Table 2, with the experimental results for CBENZ and TCE, respectively. An examination of the figures reveals that SHSDM and the DF-FPDM predictions are virtually the same and are in better agreement with the experimental BTCs than the FEHSDM. A Bi of about 8 was computed for both the compounds. The SHSDM and the DF-FPDM predictions are to be the same, as discussed earlier. These two compounds are also relatively hydrophobic.

CONCLUSIONS

The models, in general, provide convergent results and remain stable for $Pe \leq 2.5$ and $Cr \leq 1.0$. The SHSDM and the DF-FPDM predictions are virtually the same for $Bi \geq 5$. Significant difference in the predictions of these two models are observed for $Bi \leq 1$. The FEHSDM predictions are always somewhat different than those by the SHSDM and the DF-FPDM. The

FEHSDM predictions are in better agreement with the experimental BTCs for slightly hydrophobic compounds. The SHSDM and the DF-FPDM predictions are in better agreement with the experimental results for relatively hydrophobic compounds.

REFERENCES

Ball, W. P. and Roberts, P. V. (1991) Long-term sorption of halogenated organic chemicals by aquifer material. 1. Equilibrium. Environ.Sci. Technol. 25(7), 1223–1236.

Chen, T. L. and Hsu, J. T. (1987) Prediction of breakthrough curves by the application of Fast Fourier Transform. AIChE J. 33, 1387.

Cornelissen, G., Van Noort, P. C. M. and Govers, H. A. J. (1998) Mechanisms of slow desorption of organic compounds from sediments: A study using model sorbents.
Environ. Sci. Technol. 32(20), 3124–3131.

Farrell, J., Grassian, D. and Jones, M. (1999) Investigation of mechanisms contributing to slow desorption of hydrophobic organic compounds from mineral solids. Environ. Sci. Technol. 33(8), 1237–1243.

Grathwohl, P. and Reinhard, P. (1993) Desorption of trichloroethylene in aquifer material: Rate limitation at the grain scale. Environ. Sci. Technol. 27(14), 2360–2366.

Hand, D. W., Crittenden, J. C. and Thacker, W. E. (1984) Simplified model for design of fixed-bed adsorption systems. J. Environ. Eng. ASCE 110(2), 440 – 456.

Hossain, M.A. and Yonge, D.R. (1992) Finite Element Modeling of Single-Solute Activated-Carbon Adsorption. J. Envir. Eng. ASCE 118(2), 238 – 252.

Hu, Qinhong. and Brusseau, M. L. (1996) Transport of rate-limited sorbing solutes in an aggregated porous medium: A multiprocess non-ideality approach. J. Contam. Hydrol. 24 (1), 53-74.

Kleineidam, S., Runger, H., Ligouis, B. and Grathwohl, P. (1999) Organic matter facies and equilibrium sorption of phenanthrene. Environ. Sci. Technol. 33(10), 1637-1644.

Liang, S. (1984) Mathematical modeling of sorption in heterogeneous system. Ph. D. Dissertation, University of Michigan, Ann Arbor, Michigan. U.S.A.

Loehr, R. C. and Webster, M. T. (1996) Behavior of fresh vs. aged chemicals in soil. J. Soil Contaminant 5, 361–383.

Loehr, R.C., Webster, M.T. and Smith, J.R. (2000) Fate of treated and weathered hydrocarbons in soil - Long-term changes. Practice Periodical of Hazardous, Toxic and Radioactive Waste Management, ASCE, 4(2), 53-59.

Neidermeir Craig A. and Loehr Raymond C. (2005) Application of an intraparticle diffusion

model to describe the release of polyaromatic hydrocarbons from field soils.
J. Envir. Engrg. 131, 943.

Pignatello, J. J., Ferrandino, F. J. and Huang, L. Q. (1993) Elution of aged and freshly added herbicides from a soil. Environ. Sci. Technol. 27(8), 1563–1571.

Rahman, M., Amiri, F. and Worch, E. (2003) Application of the mass transfer model for describing nonequilibrium transport of HOCs through natural geosorbents.
Water Research. 37, 4673-4684.

Raghavan, N. S. and Ruthven, D. M. (1983) Numerical simulation of a fixed-bed adsorption column by the method of orthogonal collocation. AIChE J. 29, 922.

Sun, L. M. and Meunier, F. (1991) An improved finite difference method for fixed-bed multicomponent sorption. AIChE J. 37, 244.

Thacker, W.E. (1981) Modeling of activated carbon and coal gasification char adsorbents in single-solute and bisolute systems, Ph. D. Dissertation, University of Illinois at Urbana-Champaign, Urbana, Illinois, U.S.A.

Thibaud-Erkey, C., Guy, Y., Erkey, C. and Akgerman, A. (1996) Mathematical modeling of adsorption and desorption of volatile contaminants from soil: Influence of isotherm shape on adsorption and desorption profiles. Environ. Sci. Technol. 30(7), 2127-2134.

Weber, W. J., Jr. and Pirbazari, M. (1982) Adsorption of toxic and carcinogenic compounds from water. J. Am. Water Works Assoc. 74, 440 – 456.

Weber, W. J., Jr. and Digiano, F.A. (1995) Process Dynamics in Environmental Systems.John Wiley & Sons, INC. New York, U.S.A.

Worch, E. (2004) Modeling the solute transport under nonequilibrium conditions on the basis of mass transfer equations. J. Contam. Hydrol. 68, 97 – 120.

TABLES

Table 1: Model parameters obtained from Rahman et al. (2003).

Parameters	2-M-4,6-DNP	2,4,6-TCP	Phenanthrene	PCP
$v\ (cm\ s^{-1})$	6.66×10^{-3}	6.66×10^{-3}	10.61×10^{-3}	6.66×10^{-3}
$L\ (cm)$	50	50	9	50
$D^{1}\ (cm^2\ s^{-1})$	1.332×10^{-3}	1.332×10^{-3}	2.12×10^{-3}	1.332×10^{-3}
ε	0.37	0.37	0.32	0.37
$\rho_b\ (gm\ cm^{-3})$	1.68	1.68	1.79	1.68
$r\ (cm)$	0.04	0.04	0.006	0.04
$k\ (ml\ gm^{-1})$	0.008	0.022	11.6	0.60
n	1	1	1	1
$C_0\ (mg\ L^{-1})$	0.10	0.10	0.10	0.10
$k_f\ (cm\ s^{-1})$	1.47×10^{-3}	1.6×10^{-3}	8.22×10^{-3}	1.6×10^{-3}
$D_s\ (cm^2\ s^{-1})$	1.92×10^{-6}	9.6×10^{-7}	4.08×10^{-10}	8.53×10^{-8}
$k_f a_v\ (s^{-1})$	0.11	0.12	4.11	0.12
$k_s a_v\ (s^{-1})$	0.018	0.009	0.00017	0.0008

[1]D was computed by utilizing dispersivity obtained through tracer tests by Rahman et al. (2003).

Table 2: Model parameters obtained from Hu and Brusseau (1996).

Parameters	**TCE**	**CBENZ**
$v\left(cm\ s^{-1}\right)$	4.94×10^{-3}	4.58×10^{-3}
$L\left(cm\right)$	7	7
$D\left(cm^2\ s^{-1}\right)$	9.95×10^{-4}	9.25×10^{-4}
ε	0.37	0.37
$\rho_b\ \left(gm\ cm^{-3}\right)$	1.65	1.65
$r\left(cm\right)$	0.05	0.05
$k\left(ml\ gm^{-1}\right)$	0.85	1.39
n	1	1
$C_0\ \left(mg\ L^{-1}\right)$	30	100
$k_f{}^1\ \left(cm\ s^{-1}\right)$	6.66×10^{-4}	6.84×10^{-4}
$D_s{}^1\ \left(cm^2\ s^{-1}\right)$	1.75×10^{-6}	1.16×10^{-6}
$k_f a_v\ \left(s^{-1}\right)$	0.04	0.041
$k_s a_v\ \left(s^{-1}\right)$	0.011	0.007

[1] k_f and D_S were computed by using empirical correlations obtained from literature (Worch, 2004).

FIGURES

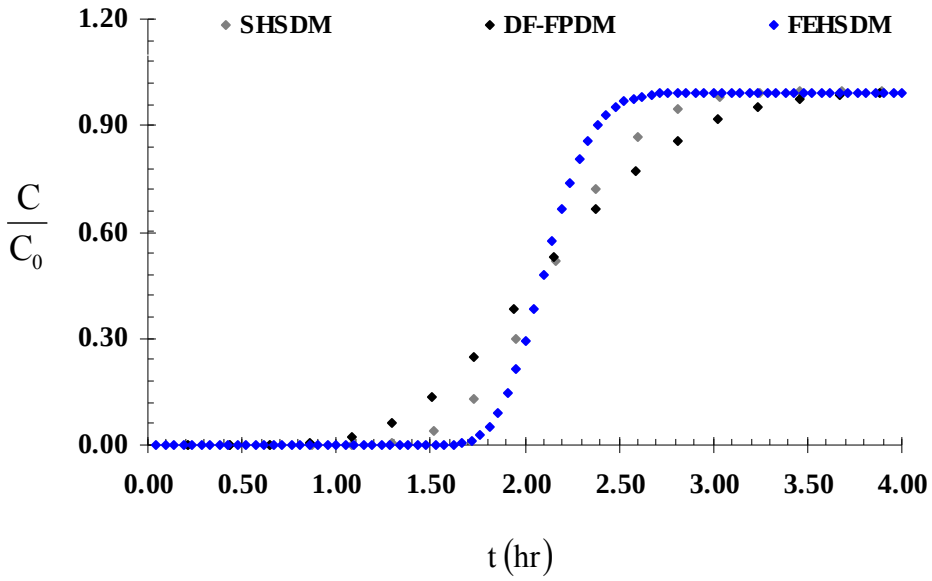

Fig. 1: Model predicted BTCs for $\mathrm{Bi} = 1$.

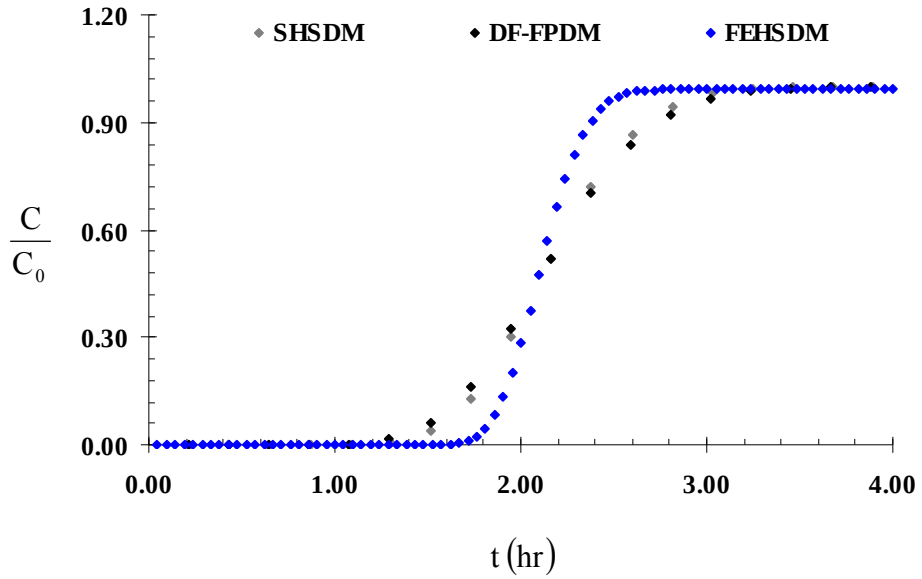

Fig. 2: Model predicted BTCs for $Bi = 5$.

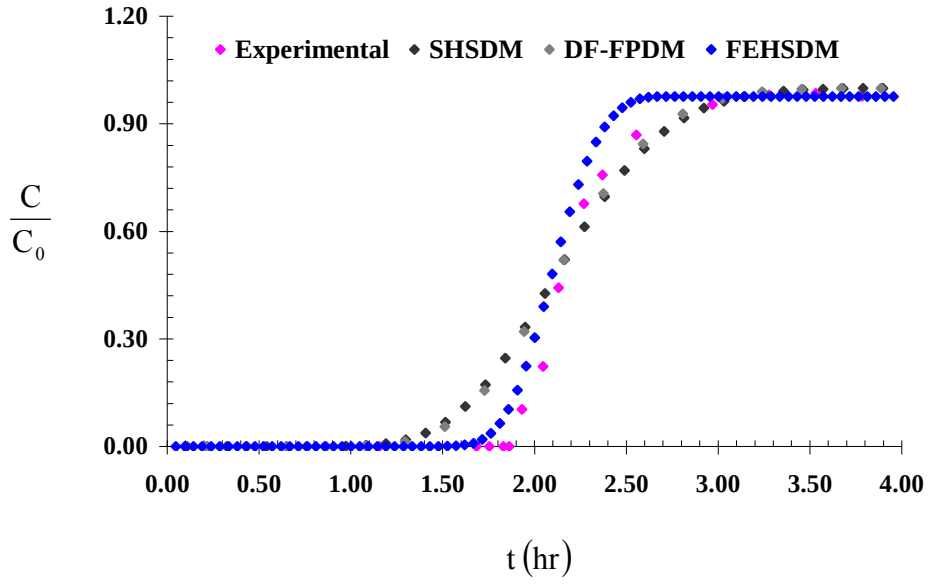

Fig. 3: Model predictions versus experimental breakthrough curve for 2-M-4,6-DNP obtained from Rahman et al. (2003).

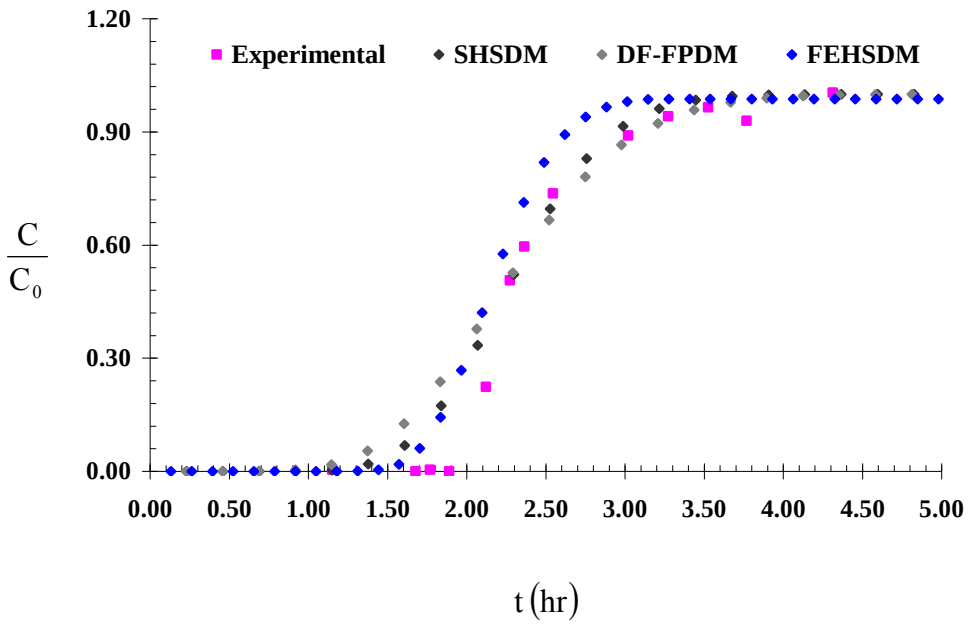

Fig. 4: Model predictions versus experimental breakthrough curve for 2-4-6,TCP obtained from Rahman et al. (2003).

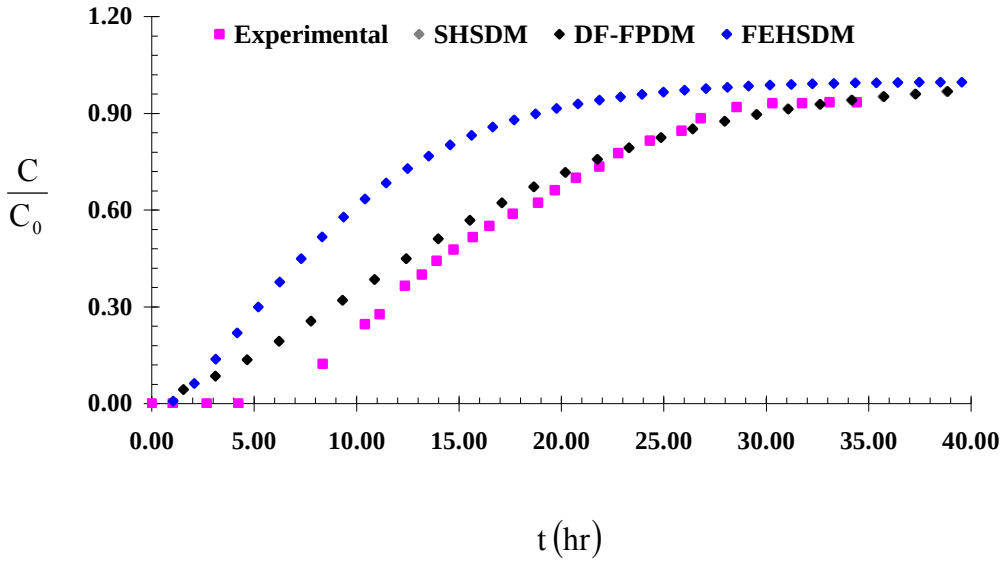

Fig. 5: Model predictions versus experimental breakthrough curve for phenanthrene obtained from Rahman et al. (2003).

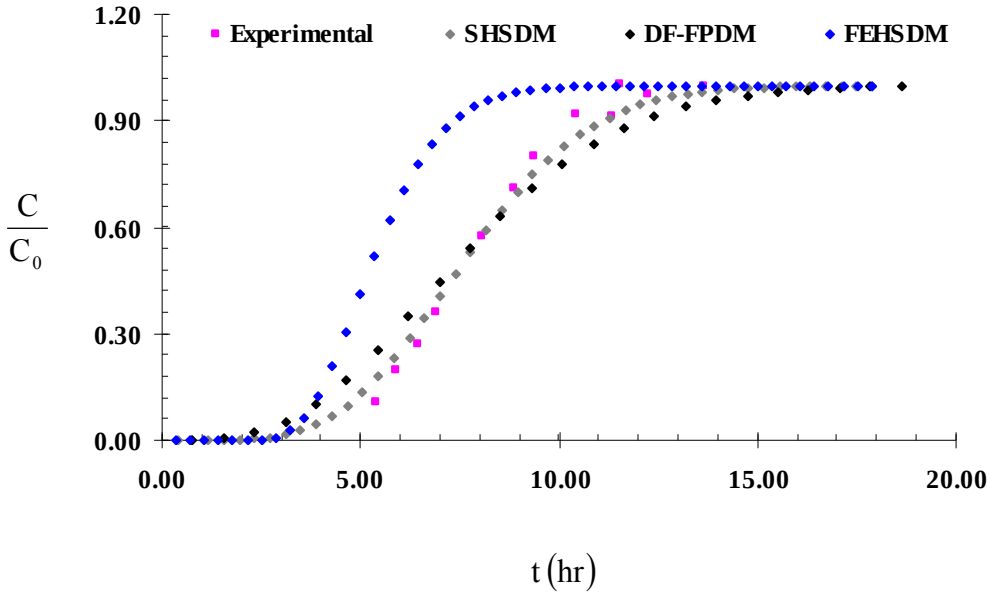

Fig. 6: Model predictions versus experimental breakthrough curve for PCP obtained from Rahman et al. (2003).

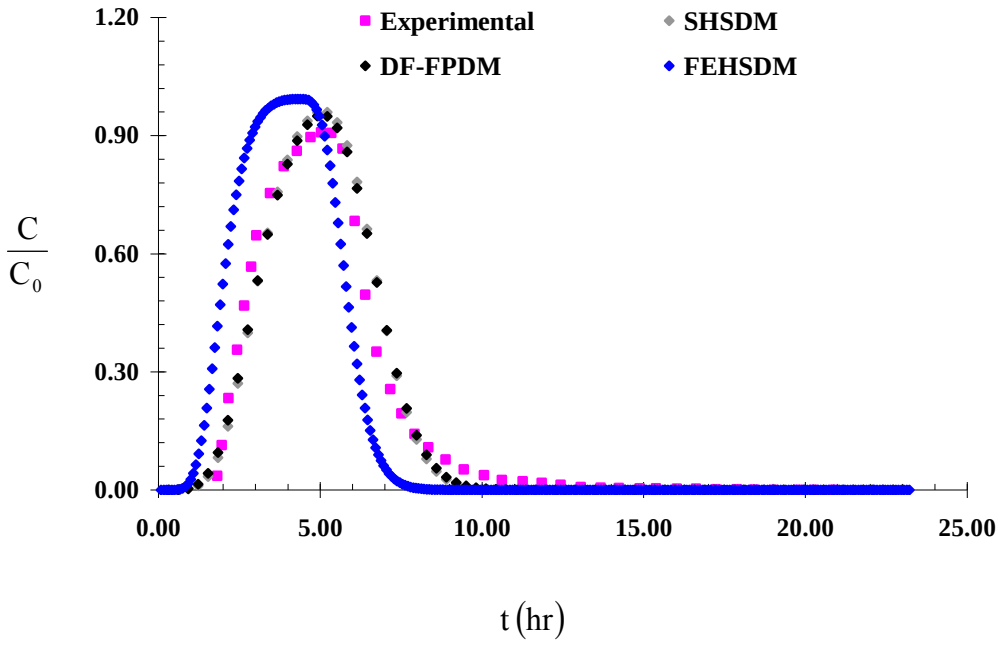

Fig. 7: Model predictions versus experimental breakthrough curve for CBENZ obtained from Hu and Brusseau (1996).

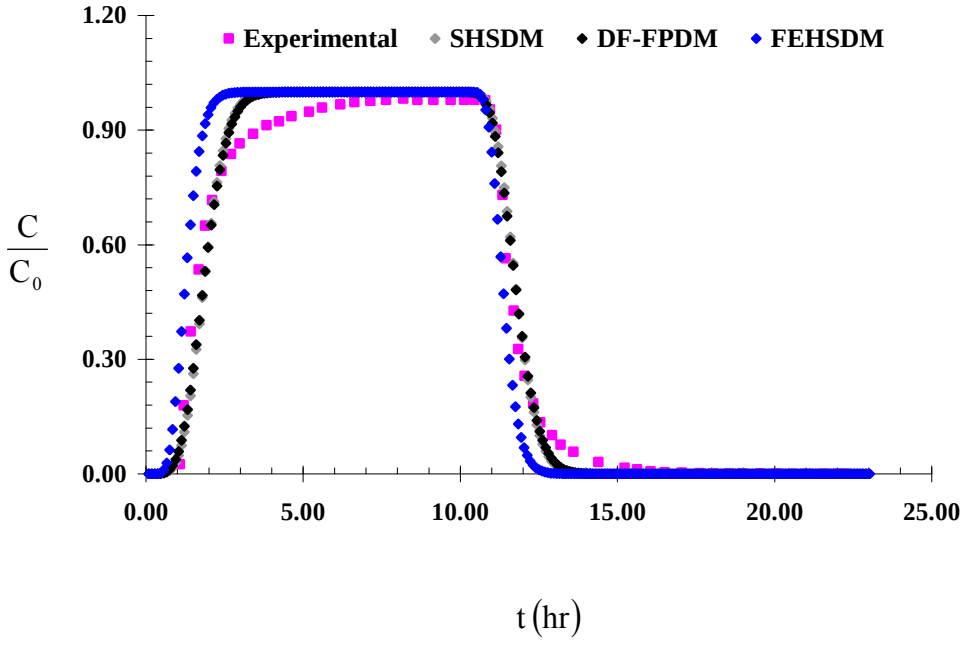

Fig. 8: Model predictions versus experimental breakthrough curve for TCE obtained from Hu and Brusseau (1996).

NOTATIONS

C = contaminant concentration in the inter-particle pore spaces $\left(ML^{-3}\right)$

C_s = concentration of contaminants in the boundary layer surrounding a particle $\left(ML^{-3}\right)$

q = concentration of the contaminant in the soil solid $\left(MM^{-1}\right)$

q_s = concentration of the contaminant on the surface of the soil solids $\left(MM^{-1}\right)$

t = time $\left(T\right)$

v = velocity of flow through the inter-particle pore spaces $\left(LT^{-1}\right)$

x = distance along the direction of the flow $\left(L\right)$

R = radius of a particle $\left(L\right)$

r = radial distance from the center of a particle $\left(L\right)$

ρ_b = bulk density of the soils $\left(ML^{-3}\right)$

ε = porosity

α = dispersivity $\left(L\right)$

D = dispersion coefficient $\left(L^2T^{-1}\right)$

k_s = intra-particle mass transfer coefficient $\left(L^2T^{-1}\right)$

a_V = mass transfer area per unit volume $\left(L^2L^{-3}\right)$

k_f = film transfer coefficient $\left(LT^{-1}\right)$